FREQUENCY STABILITY OF METHANE-STABILIZED HE-NE LASERS

Helmut Hellwig, Howard E. Bell, Peter Kartaschoff,* and James C. Bergquist†

Atomic Frequency and Time Standards Section
National Bureau of Standards
Boulder, Colorado 80302 USA

Free-running laser stabilities of 1.5×10^{-11} for the millisecond region and methane-locked stabilities of 10^{-13} for 10 s averaging time are achieved with a minimum of shock and vibration isolation in an ordinary laboratory environment. Superior stability performance is obtained with dc excitation as compared to rf excitation. The experimental setup is described in some detail.

The P(7) line of the ν_3 band of CH_4 at 3.39 μm (88 THz) is regarded as one of the most promising candidates for an accurate frequency and length reference for measurements in the infrared and visible radiation region. This line has been proposed as a successor for the present standard of length (krypton).[1] It is also proposed as a possible future unified standard for both length and time-interval,[1-3] provided its accuracy is competitive and provided that the already spectacular results in frequency synthesis in the infrared region lead to an accurate frequency comparison between the standards of time-interval and length. In view of these important possibilities we investigated the performance of CH_4-stabilized He-Ne lasers.

The design closely resembles the one described by Barger and Hall.[4] The gas cell containing CH_4 is located inside of the 60 cm optical cavity. Saturation of the absorption line results in a sharp increase in the laser output power at the center of the methane resonance. In our experiments this emission feature was typically a few percent of the total laser power, with a linewidth of about 100 kHz (line $Q \approx 10^9$). The methane pressure was about 10 m Torr (1.33 N/m^2). Coincidence of the center of the single-mode laser emission profile with the methane absorption was achieved by pressure shifting

with 4.8 torr (640 N/m^2) of ^3He. We used typically 0.2 torr (27 N/m^2) of ^{20}Ne. The capillary of the laser gain cell was 18 cm long with 3 mm inside diameter. No particular effort was made to reduce environmental disturbances. The experiments were performed in an ordinary laboratory without acoustical isolation. The apparatus was mounted on a one-half-inch steel plate which was buffered against shock and vibration from the support structure by a one-inch foam rubber pad.

In Fig. 1 we depict the measurement system. The outputs of both devices were combined with a mirror M and a beam splitter S and focussed on a diode D (Philco-Ford L4530).[5] The resultant beat was amplified in A_3, a dc amplifier with a bandwidth of 1 MHz, and counted. For on-line evaluation of the frequency stability we used a computing counter (HP5360A) which was programmed to display directly the two-sample Allan variance.[6,7]

The servo system is shown on the right side of Fig. 1. The infrared frequency was modulated by means of a piezoelectric transducer (PZT) driven at the rate ν_m from the modulation generator MG. The tuning sensitivity (fractional frequency) with our PZT was 5×10^{-9} per volt; a swing of 60 V in our PZT driver amplifier A_2 was sufficient for maintaining lock over many hours. Each laser was pre-tuned by adjustment (75 V steps) of its battery B. The frequency-lock to the methane saturated absorption was accomplished in the usual way with the phase detector PD, the integrator I, and the amplifier-filter combination F. For unambiguous measurement of the Allan variance (Figs. 2 and 3), the frequency difference between the two lasers was typically 50 kHz (locked) and 500 kHz (unlocked). In the locked case, the offset was introduced by placing a small dc bias at the input of the integrator I.

In our first series of experiments both lasers were excited with a 40-MHz radio-frequency discharge. The modulation frequency was $\nu_m = 5$ kHz. The results, normalized to one device, are depicted in Fig. 2. The upper (dashed) curve gives the free-running laser stability, the lower (solid) curve gives the locked performance.

We used dc excitation of the laser discharges in the second series of experiments and obtained improved stability performance. See Fig. 3. The modulation frequency was set at ν_m = 3 kHz. We used a cylindrical cathode of about 2 cm diameter and 5 cm long in a concentric position at the end of the discharge capillary. The electrode was made from pure aluminum. Typical discharge currents were in the range from 1.5 to 2.0 mA. Exceeding 2.0 mA caused discharge conditions which resulted in excessive amplitude noise but which did not significantly affect the frequency stability performance.

The precision confidence limit of each data point in Figs. 2 and 3 is within the precision of the drawing, except for data points at $\tau \geq 1000$ s where the confidence is only about 50 percent of the value. We were able to record stabilities as shown in Figs. 2 and 3 repeatedly and reliably. From Figs. 2 and 3 we see that the servo responds in a few tenths of a millisecond. Out to τ = 1 s, the locked stability improves as $\tau^{-1/2}$, i.e., as white frequency noise, and reaches 1.1×10^{-13} for τ = 10 s. This stability performance corresponds to a power spectrum linewidth of W $\approx$ 2 kHz as can easily be calculated from (valid for white frequency noise) $W = 2\pi\tau\nu^2\sigma^2$ where ν is the laser frequency. For time intervals greater than several seconds the locked stability deteriorates from the $\tau^{-1/2}$ dependency. There is evidence that this degradation is not inherent in the methane cell itself but rather involves the servo electronics. In particular, the RC product of the integrator was only 0.5 s. This leads to a dc servo gain of the order of 10^3 for $\tau > 0.5$ s which is insufficient to provide for a better long-term stability. We expect that a redesigned electronics with a greater integrator RC time constant will enable us to significantly extend the $\tau^{-1/2}$ stability performance.

In agreement with previous measurements[4] we also find that the frequency difference between two independent devices, i.e., the reproducibility, is better than a few parts in 10^{11}. Our stability data (for $\tau \leq 10$ s) are better than previously reported ones.[1,8,9] We believe that this is largely due to the better free-running stability of our lasers.

In comparing the results of Figs. 2 and 3 we note that the marked frequency stability improvement in the free-running laser and the resulting improvement of the methane-stabilized laser due to switching from rf to dc excitation may be the result of a quieter discharge in the case of dc excitation. We have no other explanation because the experimental setup was the same in both experiments; even the optical cavities remained unchanged.

We note that the performance of our methane-stabilized lasers as compared to other oscillators is already quite spectacular: The frequency stability from less than 1 ms out to 10 s matches or exceeds the stability of other oscillators which have been used as standard frequency sources, i.e., of hydrogen masers, cesium beam devices, crystal oscillators, etc.

We gratefully acknowledge the generous supply of information and advice from J. L. Hall and J. Levine, and the assistance in the construction of the lasers and the electronics by Miss R. Gillis.

References

*P. Kartaschoff is a National Bureau of Standards Visiting Scientist on leave from the Laboratoire Suisse de Recherches Horlogères, Neuchâtel, Switzerland.

†J. C. Bergquist is a student at the University of Colorado.

[1]H. S. Boyne, IEEE Trans. on Instr. and Meas. IM-20, 19 (1971).

[2]This would be equivalent to a definition of the speed of light.

[3]H. Hellwig and D. Halford, Proc. of the International Conf. on Precision Measurements and Fundamental Constants, Aug. 1970, in press; also available as NBS Report 9766 (17 August 1970).

[4]R. L. Barger and J. L. Hall, Phys. Rev. Letters 22, 4 (1969).

[5]Names of manufacturers are used for the sole purpose of conveying scientific and technical information, and their citation is not to be construed as an endorsement or approval of commercial products or services by the authors or by the authors' organizations.

[6]D. W. Allan, Proc. IEEE 54, 221 (1966).

[7]Detailed information about the use of the Allan variance $\sigma^2(N, T, \tau, B)$--with N = number of samples, $(T - \tau)$ = dead time, τ = averaging (sample) time, B = bandwidth--can be found in J. A. Barnes et al., IEEE Trans. on Instr. and Meas. IM-20, 105 (1971); also NBS Technical Note 394 (Oct. 1970).

[8]R. L. Barger and J. L. Hall, Proc. 23rd Annual Symposium on Frequency Control, Fort Monmouth, N.J., 306 (1969).

[9]Private communication: Recently, J. L. Hall, R. L. Barger, and G. Kramer obtained results which are comparable with ours using different techniques and a well-controlled environment; also R. L. Barger, Bull. Am. Phys. Soc., Ser. II, 16, 347 (1971); also J. L. Hall, Isfahan Symp. on Fund. and Appl. Laser Phys., Sept. 1971, unpublished.

Figure Captions

Fig. 1 Measurement system and frequency-lock servo.

Fig. 2 Frequency stability of a free-running He-Ne laser (dashed) and a CH_4-stabilized He-Ne laser (solid) using 40 MHz rf excitation. In Figs. 2 and 3 the square root of the Allan variance[6,7] $\sigma_y^2(N, T, \tau, B)$ is plotted, where $N = 2$, $T - \tau \approx 1$ ms, $B \approx 1$ MHz, and $y \equiv$ fractional frequency fluctuations. The gating of the counter was non-synchronous with the modulation frequency ν_m.

Fig. 3 Frequency stability of a free-running He-Ne laser (dashed) and a CH_4-stabilized He-Ne laser (solid) using dc excitation.

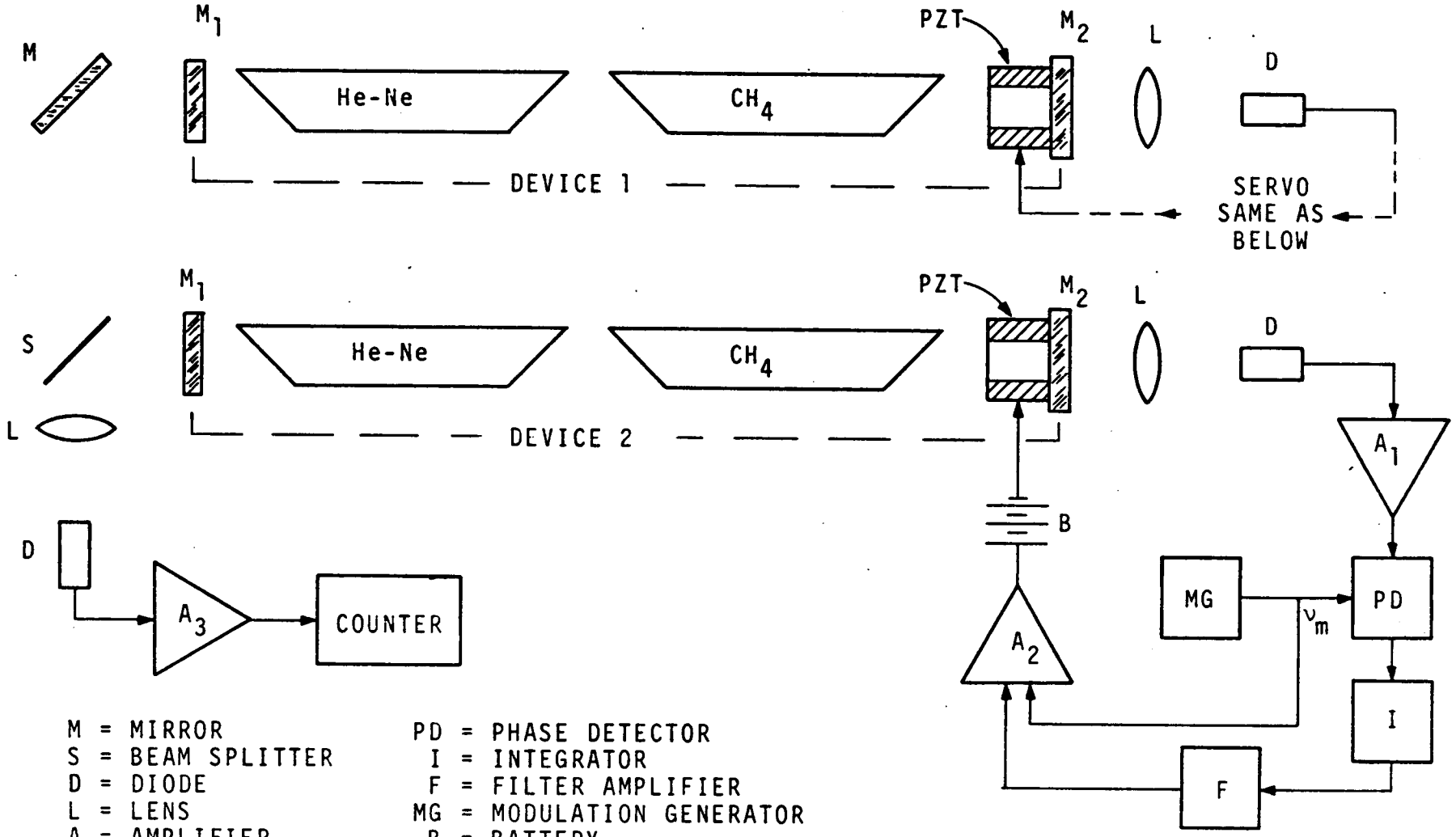
M
M1
He-Ne
CH4
PZT
M2
L
D
DEVICE 1
SERVO
SAME AS
BELOW
S
L
DEVICE 2
A1
B
A2
MG
νm
PD
I
F
D
A3
COUNTER
M = MIRROR
S = BEAM SPLITTER
D = DIODE
L = LENS
A = AMPLIFIER
PD = PHASE DETECTOR
I = INTEGRATOR
F = FILTER AMPLIFIER
MG = MODULATION GENERATOR
B = BATTERY

Fig. 1

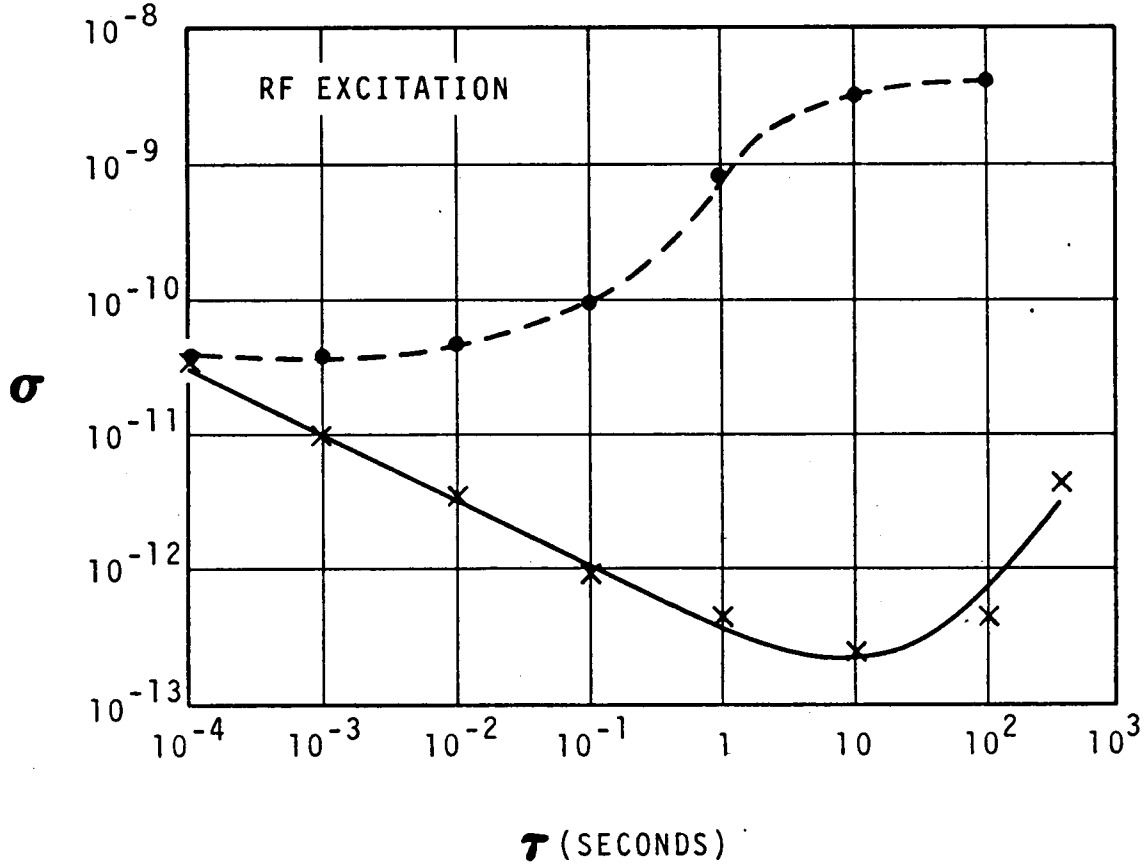
RF EXCITATION
10^{-8}
10^{-9}
10^{-10}
10^{-11}
10^{-12}
10^{-13}
σ
10^{-4}
10^{-3}
10^{-2}
10^{-1}
1
10
10^{2}
10^{3}
τ (SECONDS)

Fig. 2

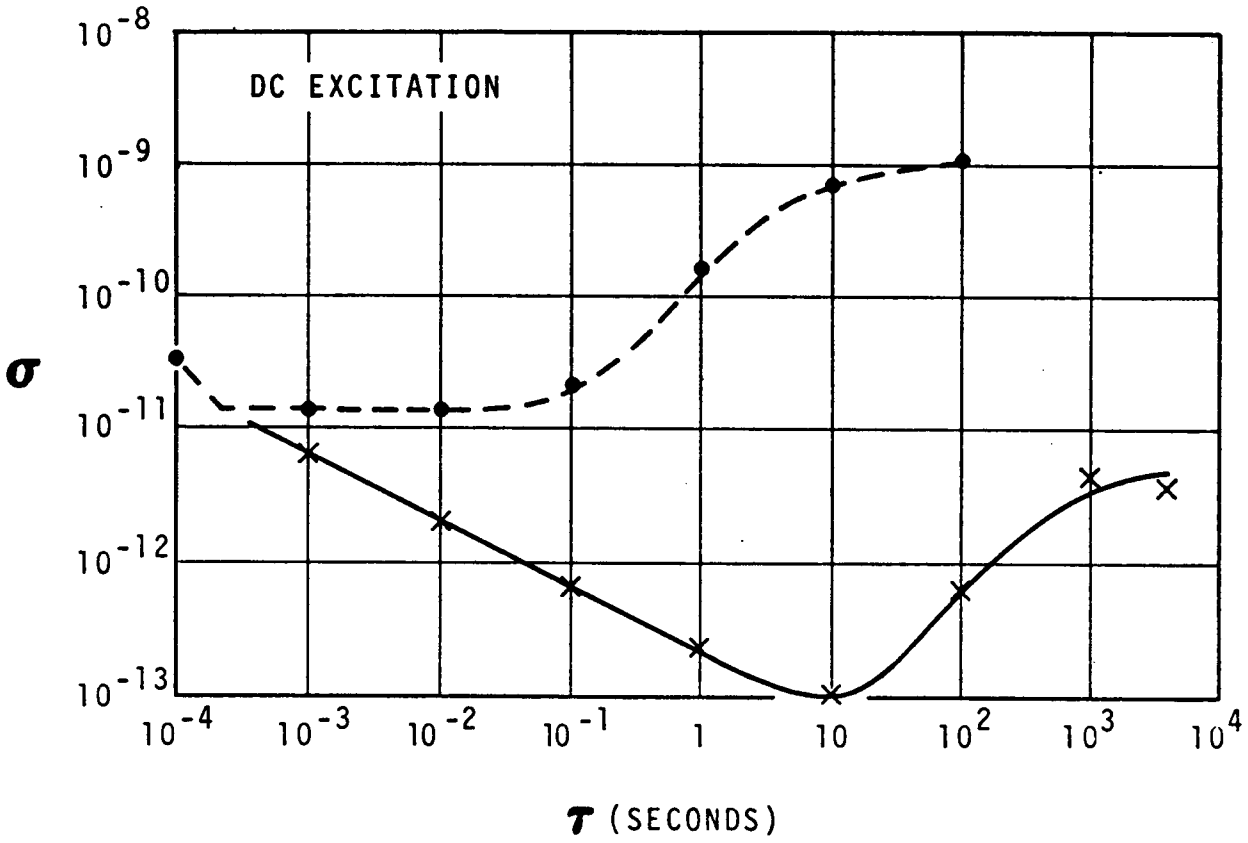
DC EXCITATION
10^{-8}
10^{-9}
10^{-10}
10^{-11}
10^{-12}
10^{-13}
σ
10^{-4}
10^{-3}
10^{-2}
10^{-1}
1
10
10^{2}
10^{3}
10^{4}
τ (SECONDS)

Fig. 3